Pergamon

Chemical Engineering Science, Vol. 50, No. 2, pp. 263–277, 1995

0009-2509/95 $9.50 + 0.00

0009-2509(94)00238-X

INFLUENCE OF THE SURFACE VISCOSITY ON THE DRAG AND TORQUE COEFFICIENTS OF A SOLID PARTICLE IN A THIN LIQUID LAYER

K. D. DANOV
Laboratory of Thermodynamics and Physico-Chemical Hydrodynamics, Faculty of Chemistry, University of Sofia, J. Bourchier Ave. 1, Sofia 1126, Bulgaria

and

R. AUST,* F. DURST and U. LANGE
Lehrstuhl für Strömungsmechanik, Universität Erlangen-Nürnberg, Cauerstr. 4, D-91058 Erlangen, Germany

(*Received* 4 *May* 1994; *accepted in revised form* 25 *July* 1994)

Abstract—The present paper provides a short literature survey of the treatment of particle motion in fluids as a basis of the author's own work in this field. The work relates to the motion of a small solid particle inside a thin liquid film. The particle motion is treated numerically to provide information of interest to thin film liquid coating. The numerical computations yield information on the local velocity and pressure distributions, but also integral information expressed in drag and torque coefficients. The computations are carried out for stationary flows of low Reynolds and capillary numbers and results are presented for different values of surface dilatation and shear viscosities. Translational and rotational motions of the particle are considered by integrating the resultant second-order partial differential equation with an alternating direct implicit method. The numerical results reveal in all cases the strong influence of the surface viscosity on the motion of the solid particle in the viscous liquid layer when the radius of the particle is of the same order of magnitude as the thickness of the liquid film or when the particle is close to the liquid–gas interface.

1. INTRODUCTION

The motion of a single particle in a fluid has fascinated fluid dynamists for more than a century and analytical treatments have been put forward by many researchers. Stokes (1851) derived the formula for the friction force exerted on a spherical particle moving with constant velocity in an unlimited incompressible viscous fluid. Kirchhoff (1876) gave the solution for a spherical particle slowly rotating in an unbounded fluid with the same fluid properties as employed by Stokes (1851). Rybczynski (1911) and Hadamard (1911) generalised Stokes' (1851) (low-Reynolds number) solution for the settling velocity of a solid sphere and derived the solution for the case of a spherical fluid droplet. However, experiments [cf. Lebedev (1916) and Silvey (1916)] performed shortly afterwards revealed that fluid droplets of sufficiently small radius settled as if they were solid spheres, obeying Stoke's original formula. Boussinesq (1913), in an attempt to resolve this discrepancy between theory and experiment, postulated the existence of a surface viscosity, conceived as the two-dimensional equivalent of the conventional three-dimensional viscosity possessed by bulk-fluid phases. The solution for a neutrally buoyant rigid sphere suspended in a homogenous shear flow that extends to infinity was probably first obtained by Einstein (1956) in his theory of the viscosity of particle suspensions.

The theory of Einstein (1956) was extended by Jeffery (1922) to nonspherical particles, where a new feature arises due to the orientation of the particle relative to the principal axes of shear. Jeffery's (1922) classic analysis of the periodic rotation of an ellipsoid of revolution suspended in a simple shearing motion of a viscous fluid. The status of knowledge in this field was summarised and theory and experiment were compared by Goldsmith and Mason (1967).

Up to the mid-1960s a great deal of work was done in obtaining first- and higher-order wall corrections for particles in flows that are bounded by plane or cylindrical walls [cf. Happel and Brenner (1965)]. The force and torque exerted on the particle were expressed in a power series according to a/l, where a is the particle radius and l is the distance between the centre of the particle and the wall. Following this idea, Lorentz (1906) derived the motion of a sphere perpendicular to a flat wall up to a/l. Faxén (1921) developed the method of reflection for a sphere moving between two parallel planes in a viscous fluid. Using his method Wakiya (1956) considered the cases of motion in Poiseuille- and Couette-flow. As was pointed out by Hetsroni (1982), the method employed by Wakiya (1956) does not yield physically correct results for

*Author to whom correspondence should be addressed.

small distances from the wall. An important step forward towards a solution of the particle motion near a wall was made by the theoretical work of Dean and O'Neill (1963). They showed that the force and the torque acting on a spherical particle, moving in a viscous fluid at an arbitrary distance in a plane parallel to the wall, can be accurately determined. The limiting behaviour when the sphere is almost in contact with the wall was obtained rigorously by O'Neill and Stewartson (1967), Goldman *et al.* (1967) and Cooley and O'Neill (1968). Instead of the exact solution of the problem these authors derived asymptotic formulae for the force and torque and corrected some inaccuracies made in the previous work of Dean and O'Neill (1963) and O'Neill (1964). Ranger (1978) considered the problem of a disk rotating with axial symmetry in the presence of a flat interface separating two immiscible fluids of different viscosities. O'Neill and Ranger (1979) derived the exact solution for the velocity field induced by a sphere rotating close to the interface between two immiscible viscous fluids. Shapira and Haber (1988, 1990) studied the low Reynolds number hydrodynamics of a droplet moving in a quiescent fluid between two parallel plates and the hydrodynamic interaction between a droplet immersed in Couette flow and the containing walls.

For many years the Boussinesq (1913) solution, based upon his surface viscosity postulate, was accepted as the basis to explain the anomalous droplet settling-velocity results, encouraging the development of a plenteousness of instruments for measuring surface viscosity, as well as other rheological properties of fluid interfaces [cf. Joly (1964)]. The work by Sternling and Scriven (1959), together with Scriven's (1960) paper, wherein Boussinesq's theory was generalised to material interfaces of arbitrary curvature, marked a turning point toward today's modern understanding of interfacial rheology [cf. Edwards *et al.* (1991)].

The effects of bulk and interfacial rheological properties and surfactant adsorption–desorption kinetics on the rate of drainage of foam and emulsion films was studied by Zapryanov *et al.* (1983) and Malhotra and Wasan (1987). The effects of Gibbs elasticity and surface viscosity upon the drag coefficient of an emulsion droplet in adsorption controlled Marangoni flow was presented by Levich (1962) and Edwards *et al.* (1991). The effect of Gibbs elasticity is usually neglected when the concentration of insoluble surfactants are small or the diffusion of soluble surfactants is fast. In these cases we can calculate the flow in the frame of Newtonian volume and surface rheology.

One of the most convenient numerical method for solving this class of problems is the method of finite elements. It was utilised by Brebbia (1978) and Fletcher (1984) for solving the problem of the motion of a cylinder between two walls. The latter problem, however, is two-dimensional, in contrast to a spherical particle (instead of cylinder) moving between two interfaces. That is why the solution proposed by Brebbia (1978) and Fletcher (1984, 1991b) is not applicable to the problem considered here, which is essentially three-dimensional. To complete the above given summary of the literature on studies of particle motion in fluids, some of the more recent publications need to be mentioned. The general approach, along with some important technological and biological applications, is considered in several monographs [cf. Hunter (1987, 1989), Russel *et al.* (1989)]. The hydrodynamics of suspensions containing solid particles was developed by several authors [cf. the review of Davis (1993), and the papers of Brenner (1973), Brenner and Leal (1982), Uijttewaal (1993), Uijttewaal *et al.* (1993), as well as the book of Kim and Karrila (1991)]. Experimentally gained rheological results show that the behaviour of hydrosols containing solid and fluid colloid particles can be rather different. The differences mainly arise from the interfacial fluidity. There are two types of viscosity behaviour: shear and dilatational. In real emulsion and microemulsion systems and in thin liquid films containing particles (defects) one can distinguish also two types of elasticity (shear and dilatational). To investigate theoretically these properties it is necessary to solve the drag and torque coefficients of an individual particle.

The present paper discusses the problem for determining the drag force and torque exerted on a solid particle in a viscous liquid layer for low Reynolds- and capillary numbers when the free surfaces-excess pressure tensor obeys the Boussinesq (1913) and Scriven (1960) constitutive law for a Newtonian interface. In thin film coating and in many other cases involving suspensions and emulsions, the particles of interest have a diameter of about 1 μm or less and the relative velocity is of the order of a few cm/s or less. Hence, for liquids such as water or commonly used solvents, the assumption of low Reynolds- and capillary numbers holds in most practical important cases.

It is proved in detail in Section 2 that the problem for Stokes' flow in a cylindrical coordinate system of revolution can be reduced from three-dimensions to two-dimensions. The presented problem has no analytical solution because there is no analytical conformal transformation of the considered region into a square. In Section 3 Stokes' equations and boundary conditions are transformed to an equivalent well-defined system of second-order partial differential equations with known boundary conditions using the "two vorticities-one velocity" formulation. A numerical procedure is invented based on the alternating direction implicit (ADI) method in Section 4. Using this procedure the drag force, torque coefficients, velocity and pressure distribution are obtained in Section 5 for all elementary motions which are components of the stationary velocity and pressure distribution. The numerical results reveal the strong dependence of the surface viscosity numbers on the motion (rotation and translation) of the solid particle in the viscous liquid layer when the radius of the particle is of the same order of magnitude as the thickness of the liquid film or when the particle is close to the surface.

2. DESCRIPTION OF THE MODEL

2.1. *Basic equations and boundary conditions*

Let us consider a solid spherical particle with radius a, performing either a translational motion along the Oy axis or a rotation around the Ox axis. (It can be in a state of rest as well.) The particle is immersed in a viscous fluid between two parallel viscous interfaces S_1 and S_2 [see Fig. 1(a)]. It is supposed in all cases that the deformations of the interfaces S_1 and S_2 are small [i.e. the interface capillary numbers, defined by eq. (10), are small] and that the stationary motions are slow (small Reynolds number). Therefore, the flow is considered as a viscous, incompressible creeping motion which obeys the Stokes' equations:

$$\nabla \cdot \mathbf{v} = 0, \qquad \eta \nabla^2 \mathbf{v} = \nabla p \tag{1}$$

where p is the pressure, η is the dynamic viscosity and $\mathbf{v}$ is the local fluid velocity.

The boundary condition on the surface S_0 of the solid particle is [see Fig. 1(a)]

$$\mathbf{v} = \mathbf{v}_0 \quad \text{at } S_0 \tag{2}$$

where $\mathbf{v}_0$ is the velocity of the particle. In order to account for the influence of the surfactants, we consider the Boussinesq–Scriven constitutive law for the Newtonian interfaces S_1 and S_2. Then the Newtonian surface-excess stress tensor $\mathbf{S}$ can be defined in the following form [cf. Scriven (1960) and Edwards *et al.* (1991)]

$$\mathbf{S} = \sigma \mathbf{I}_s + (\eta_d - \eta_{sh})(\mathbf{I}_s : \mathbf{D}_s)\mathbf{I}_s + 2\eta_{sh}\mathbf{D}_s. \tag{3}$$

In eq. (3) σ is the thermodynamic interfacial tension, η_{sh} and η_d are, respectively, the interfacial shear and dilatational viscosities at a given point of the interface, $\mathbf{I}_s$ is the unit surface idemfactor. Thus $\mathbf{D}_s$, which constitutes the symmetric portion of the surface velocity dyadic

$$\mathbf{D}_s = \frac{1}{2}\left[(\nabla_s \mathbf{v}_s)\cdot \mathbf{I}_s + \mathbf{I}_s \cdot (\nabla_s \mathbf{v}_s)^{\mathrm{T}}\right] \tag{4}$$

represents the rate of relative displacement of surface points, where $\mathbf{v}_s$ is the surface velocity and ∇_s is the surface gradient. Equations (3) and (4) are the two-dimensional analogs to the comparable expressions for the bulk phase pressure tensor and the three-dimensional rate of deformation tensor respectively. Because in all practical circumstances the surface-excess mass density is small compared to the bulk-phase mass density, the equation for the interfacial momentum transport reduces to the form

$$\nabla_s \cdot \mathbf{S} = \mathbf{n}_s \cdot \langle \mathbf{P} \rangle \tag{5}$$

where $\mathbf{n}_s$ is the unit normal to the liquid–gas interface and $\langle \mathbf{P} \rangle$ is the jump of the volume stress tensor $\mathbf{P}$

$$\mathbf{P} = -p\mathbf{I} + \eta[\nabla \mathbf{v} + (\nabla \mathbf{v})^{\mathrm{T}}] \tag{6}$$

at the liquid–gas interface. It provides the explicit interfacial stress boundary condition for a Newtonian interface.

The resultant force $\mathbf{F}$, due to the stresses, exerted by the surrounding fluid on the surface of the spherical solid particle S_0 and the torque $\mathbf{M}$ experienced by the body surface are [cf. Happel and Brenner (1965)]

$$\mathbf{F} = \int_{S_0} \mathbf{P}\cdot \mathbf{n}\, dS_0, \qquad \mathbf{M} = \int_{S_0} (\mathbf{r}_0 \times \mathbf{P})\cdot \mathbf{n}\, dS_0 \tag{7}$$

where $\mathbf{r}_0$ is the position vector and $\mathbf{n}$ is the outward pointing unit normal. Since the problem under consideration is linear for small capillary and Reynolds numbers, the stationary particle motion in the liquid flow can be presented as a superposition of translational and rotational elemenıary motions. Hence, the hydrodynamic drag forces and torques of particle translation and rotation are counterbalanced by those connected with the external forces

$$\mathbf{F}_m + \mathbf{F}_r + \mathbf{F}_b = \mathbf{0}, \qquad \mathbf{M}_m + \mathbf{M}_r = \mathbf{0} \tag{8}$$

where $\mathbf{F}_m$, $\mathbf{F}_r$ and $\mathbf{M}_m$, $\mathbf{M}_r$ are, respectively, the drag force and the torque of translation and rotation and $\mathbf{F}_b$ is the external force (for example buoyancy force parallel to the undisturbed surfaces).

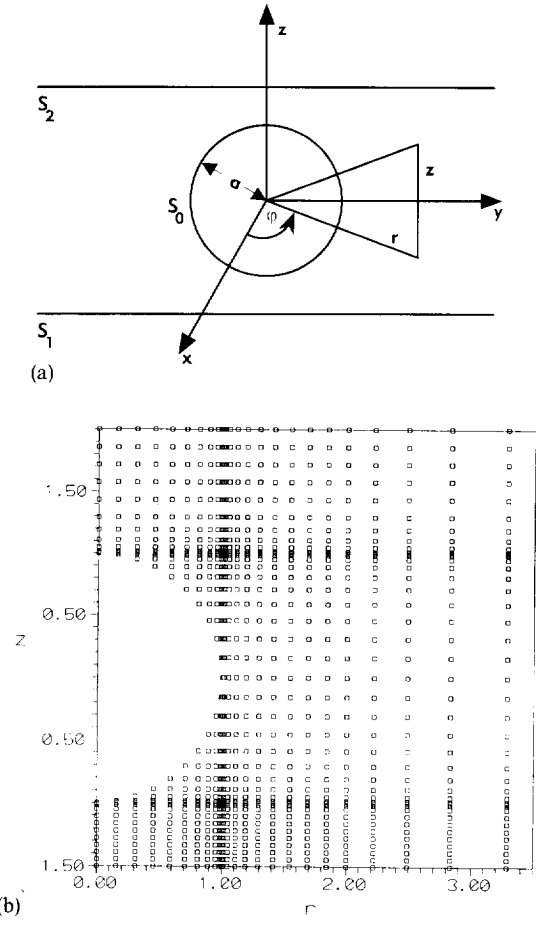

Fig. 1. (a) Geometry of the system. (b) Mapping of the numerical grid from the curvilinear system of revolution onto the r, z-plane.

2.2. *Fourier separation ansatz and parameters*

We denote $Oxyz$ as a system of Cartesian coordinates. With respect to this system, φ is a meridian

angle, any plane for which φ is constant a meridian plane, r and z are, respectively, radial and vertical coordinates in a cylindrical coordinate system $Or\varphi z$ [see Fig 1(a)]. Dimensionless variables along the r- and z-coordinate are introduced by scaling with the particle radius a. Then the equations of the liquid–gas interfaces and particle surface can be written as

$$S_k:\ z = z_k + Q_k h_k(r)\sin\varphi \quad (k = 1, 2),$$
$$S_0:\ r^2 + z^2 = 1 \tag{9}$$

where z_1 and z_2 are the vertical coordinates of the planes, Q_1 and Q_2 are the capillary numbers, defined by

$$Q_k = \frac{\eta V_*}{\sigma_k} \quad (k = 1, 2) \tag{10}$$

h_1 and h_2 are the disturbances of the lower and upper liquid–gas interfaces, and σ_1 and σ_2 are the lower and upper interface tensions. For slow motions the characteristical velocity V_* is small and the capillary numbers are small parameters, e.g. for water solution the capillary number is equal to one when the relative velocity of the particle is about 72 m/s.

All the cases considered above have such linearized boundary conditions for the elementary motions so that the solution of eqs (1)–(6) contain only one mode of the Fourier expansion. Therefore, the dimensionless bulk velocity components R, F and Z and the dimensionless pressure P can be presented in the following general form:

$$v_r = V_* R(r, z)\sin\varphi, \qquad v_\varphi = V_* F(r, z)\cos\varphi$$
$$v_z = V_* Z(r, z)\sin\varphi, \qquad p = \frac{\eta V_*}{a} P(r, z)\sin\varphi. \tag{11}$$

The characteristic velocity V_* is the relative velocity for the translational motion and ωa, with ω being angular velocity, is the rotational motion. Insertion of the ansatz (11) into the flow equation (1) and the application of the boundary conditions (2)–(5) yields a two-dimensional system of partial differential equations for the unknowns R, F, Z, P and S_k. However, a straightforward attempt to solve this system of equations leads to computational difficulties connected with the specific form of the tangential components of the linearized stress boundary conditions for the lower and upper liquid interfaces. This reduces through the ansatz to a system of second-order differential equations:

$$(-1)^k \frac{\partial R}{\partial z} = (K_k + E_k)\frac{\partial}{\partial r}\left(\frac{\partial R}{\partial r} + \frac{R}{r} - \frac{F}{r}\right) + E_k\left(\frac{1}{r}\frac{\partial F}{\partial r} + \frac{F}{r^2} - \frac{R}{r^2}\right)$$
$$(-1)^k \frac{\partial F}{\partial z} = E_k \frac{\partial}{\partial r}\left(\frac{\partial F}{\partial r} + \frac{F}{r} - \frac{R}{r}\right) + (K_k + E_k)\left(\frac{1}{r}\frac{\partial R}{\partial r} + \frac{R}{r^2} - \frac{F}{r^2}\right) \tag{12}$$

$$Z = 0 \quad \text{at } S_k \ (k = 1, 2)$$

where K_1 and K_2 are dilatational viscosity numbers, E_1 and E_2 are shear viscosity numbers on the lower and upper liquid–gas interfaces, defined by

$$E_k = \frac{\eta_{sh,k}}{\eta a}, \quad K_k = \frac{\eta_{d,k}}{\eta a} \qquad (k = 1, 2). \tag{13}$$

These computational difficulties, which are discussed by Fletcher (1991a, b), can be avoided by the "two vorticities—one velocity" formulation outlined in the next section. Concluding this section, we point out that, by substitution of eq. (11) into eq. (7), the drag force **F** and torque **M** can be written in the form

$$F_x = 0 \qquad F_y = f\pi\eta a V_*, \qquad F_z = 0$$
$$M_x = m\pi\eta a^2 V_*, \qquad M_y = 0, \qquad M_z = 0 \tag{14}$$

where the dimensionless drag coefficient f is

$$f = \int_0^\pi \left(-P + \frac{\partial R}{\partial r} + \frac{\partial F}{\partial r} - \frac{\partial Z}{\partial z}\right)\sin^2\theta\,\mathrm{d}\theta + \int_0^\pi \left(\sin\theta\frac{\partial R}{\partial z} + \sin\theta\frac{\partial Z}{\partial r} + \sin\theta\frac{\partial F}{\partial z} + Z\right) \times \cos\theta\,\mathrm{d}\theta \tag{15}$$

and m is the dimensionless torque coefficient, determined by

$$m = \int_0^\pi \left[\left(\frac{\partial R}{\partial z} + \frac{\partial Z}{\partial r}\right)\sin\theta + \left(3\frac{\partial Z}{\partial z} - \frac{\partial F}{\partial r}\right)\cos\theta\right] \times \sin^2\theta\,\mathrm{d}\theta - \int_0^\pi \left[\left(\frac{\partial R}{\partial z} + \frac{\partial Z}{\partial r} + \frac{\partial F}{\partial z}\right) \times \sin\theta + Z\right]\cos^2\theta\,\mathrm{d}\theta. \tag{16}$$

The integration of (15) and (16) is performed along the boundary of the particle $r = \sin\theta$, $z = \cos\theta$. It is interesting to note that in this cases the drag force in the x and z directions is zero and that only the x component of the torque remains. In the case of a spherical particle moving with constant relative (translation) velocity in an unlimited incompressible viscous fluid we obtain the well-known Stokes' (1851) formula, i.e. $f = 6$ and $m = 0$. In the case of rotating a spherical particle with a constant angular velocity with respect to the Ox axis in unlimited fluid the solutions (19), (20) give the Kirchhoff's (1876) formulae $f = 0$ and $m = 8$.

3. "TWO VORTICITIES–ONE VELOCITY" FORMULATION OF THE PROBLEM

After eliminating the pressure from Stokes' equations one obtains a general equation for vorticity

$$\nabla\times\nabla\times\nabla\times\mathbf{v} = \mathbf{0}. \tag{17}$$

Let the functions ζ and ψ be connected with the r and z components of the vorticity vector with the following expressions:

$$\psi = \frac{\partial}{\partial r}(rF) - R, \qquad \zeta = \frac{\partial}{\partial z}(rF) - Z. \tag{18}$$

After substituting in eq. (17) the definitions (11) and (18) we can derive the following system of second-order differential equations:

$$\frac{\partial^2\psi}{\partial r^2}-\frac{1}{r}\frac{\partial\psi}{\partial r}+\frac{\partial^2\psi}{\partial z^2}=0$$
$$\frac{\partial^2\zeta}{\partial r^2}+\frac{1}{r}\frac{\partial\zeta}{\partial r}+\frac{\partial^2\zeta}{\partial z^2}-\frac{\zeta}{r^2}-\frac{2}{r}\frac{\partial\psi}{\partial z}=0 \tag{19}$$

for the functions ζ and ψ. From (11) and (18) the equation of continuity of (1) can be written in the form

$$\frac{\partial^2F}{\partial r^2}+\frac{3}{r}\frac{\partial F}{\partial r}+\frac{\partial^2F}{\partial z^2}-\frac{1}{r}\frac{\partial\psi}{\partial r}-\frac{\psi}{r^2}-\frac{1}{r}\frac{\partial\zeta}{\partial z}=0. \tag{20}$$

This is a second-order differential equation for the first Fourier mode of the φ velocity component F. By use of definition (18) one can compute the axial and radial components Z and R. Finally, the pressure is derived from (1), (18) and (20) to be

$$P=\frac{\partial\psi}{\partial r}-\frac{\psi}{r}+\frac{\partial\zeta}{\partial z}. \tag{21}$$

For solving the system (19), (20), it is necessary to transform the boundary conditions of the problem. At first from eqs (12) and (18) we may calculate the tangential stress and kinematics boundary conditions in the "two vorticity-one velocity" formulation. The final form of these conditions on the liquid–gas interfaces are

$$(-1)^k\frac{\partial F}{\partial z}=(K_k+E_k)\left(\frac{\partial^2F}{\partial r^2}+\frac{3}{r}\frac{\partial F}{\partial r}\right)-\frac{K_k}{r}\frac{\partial\psi}{\partial r}-(K_k+2E_k)\frac{\psi}{r^2}$$
$$(-1)^k\frac{\partial\psi}{\partial z}=E_k\left(\frac{\partial^2\psi}{\partial r^2}-\frac{1}{r}\frac{\partial\psi}{\partial r}\right) \tag{22}$$
$$\frac{\partial}{\partial z}(rF)=\zeta \quad \text{at } S_k \ (k=1,2).$$

They represent a non-homogeneous system of second-order differential equations for F and ψ. From eqs (19) and (20), one can obtain the boundary conditions on the axis of the revolution

$$\frac{\partial F}{\partial r}=0, \quad \psi=0, \quad \zeta=0 \qquad \text{at } r=0. \tag{23}$$

At infinity the values of all functions F, ζ and ψ go to zero. Equations (2) and (22) give the Neuman boundary condition at the solid particle surface.

4. NUMERICAL METHOD FOR SOLVING THE PROBLEM

Different numerical methods for solving similar problems are proposed in literature [cf. Brebbia (1978), Fletcher (1984, 1991a, b)]. We use the Alternating Direction Implicit (ADI) method to solve the resultant set of equations. Let Φ^0 be the value of functions at the time t_0, Φ^+- the value of functions at the time $t_0+\delta t/2$, Φ^1- at $t_0+\delta t$. Then the linear equation

$$\frac{\partial\Phi}{\partial t}=L_r[\Phi]+L_z[\Phi] \tag{24}$$

in the first half time step yields

$$\frac{\Phi^+}{\delta t/2}-L_r[\Phi^+]=\frac{\Phi^0}{\delta t/2}+L_z[\Phi^0] \tag{25}$$

and in the second half time step it results in

$$\frac{\Phi^1}{\delta t/2}-L_z[\Phi^1]=\frac{2\Phi^+-\Phi^0}{\delta t/2}-L_z[\Phi^0]. \tag{26}$$

In eqs (25) and (26) the linear operators L_r and L_z consist only of the derivatives of r and z, respectively. The numerical scheme gives the second-order time interpolation. The time iteration step are repeated until reaching the numerical stationary values of the functions. In our case at every half step the problem is to be solved by two stages because the boundary conditions (22) contain derivatives with respect to r and z as well.

At $t_0+\delta t/2$ the first iteration step leads to a second-order system of equations for F^+ and ψ^+ in the volume of the film

$$\frac{F^+}{\delta t/2}-\left(\frac{\partial^2F^+}{\partial r^2}+\frac{3}{r}\frac{\partial F^+}{\partial r}-\frac{1}{r}\frac{\partial\psi^+}{\partial r}-\frac{\psi^+}{r^2}\right)$$
$$=\frac{F^0}{\delta t/2}+\left(\frac{\partial^2F^0}{\partial z^2}-\frac{1}{r}\frac{\partial\zeta^0}{\partial z}\right) \tag{27}$$
$$\frac{\psi^+}{\delta t/2}-\left(\frac{\partial^2\psi^+}{\partial r^2}-\frac{1}{r}\frac{\partial\psi^+}{\partial r}\right)=\frac{\psi^0}{\delta t/2}+\left(\frac{\partial^2\psi^0}{\partial z^2}\right)$$

with the usual boundary conditions on the axis of revolution, at infinity and on the spherical surface. The boundary conditions on the liquid–gas interfaces reduce to the following second-order system of equations:

$$\frac{\psi^+}{\delta t/2}-\left[E_k\left(\frac{\partial^2\psi^+}{\partial r^2}-\frac{1}{r}\frac{\partial\psi^+}{\partial r}\right)\right]=\frac{\psi^0}{\delta t/2}-(-1)^k\left(\frac{\partial\psi^0}{\partial z}\right)$$
$$\frac{F^+}{\delta t/2}-\left[(K_k+E_k)\left(\frac{\partial^2F^+}{\partial r^2}+\frac{3}{r}\frac{\partial F^+}{\partial r}\right)\right. \tag{28}$$
$$\left.-\frac{K_k}{r}\frac{\partial\psi^+}{\partial r}-(K_k+2E_k)\frac{\psi^+}{r^2}\right]=\frac{F^0}{\delta t/2}-(-1)^k\left(\frac{\partial F^0}{\partial z}\right).$$

At $t_0+\delta t/2$ the second iteration step gives a second-order equation for ζ^+ in the volume of the film

$$\frac{\zeta^+}{\delta t/2}-\left(\frac{\partial^2\zeta^+}{\partial r^2}+\frac{1}{r}\frac{\partial\zeta^+}{\partial r}-\frac{\zeta^+}{r^2}\right)=\frac{\zeta^0}{\delta t/2}$$
$$+\left(\frac{\partial^2\zeta^0}{\partial z^2}\right)-\frac{2}{r}\frac{\partial\psi^+}{\partial z} \tag{29}$$

where the values of the function ψ^+ are already determined by eqs (27) and (28), with Dirichlet boundary conditions on the solid surface and at the liquid–gas interfaces, where the values of the function F^+ are already determined by eqs (27) and (28). Equations (27)–(29) are solved numerical using the second-order interpolation of the functions in r direction and a modified Thomas band matrix method [cf. Jennings (1977)].

The third iteration step at $t_0+\delta t$ computes for other combination of the functions $-F^1$ and ζ^1 in

the volume of the film. In this case the system of equations has the following form:

$$\frac{\zeta^1}{\delta t/2} - \left(\frac{\partial^2 \zeta^1}{\partial z^2}\right) = \frac{2\zeta^+ - \zeta^0}{\delta t/2} - \left(\frac{\partial^2 \zeta^0}{\partial z^2}\right) \tag{30}$$

$$\frac{F^1}{\delta t/2} - \left(\frac{\partial^2 F^1}{\partial z^2} - \frac{1}{r}\frac{\partial \zeta^1}{\partial z}\right) = \frac{2F^+ - F^0}{\delta t/2} - \left(\frac{\partial^2 F^0}{\partial z^2} - \frac{1}{r}\frac{\partial \zeta^0}{\partial z}\right)$$

with the usual boundary conditions on the axis of revolution and on the spherical surface. The boundary conditions on the liquid–gas interfaces have the following form:

$$\frac{F^1}{\delta t/2} - (-1)^k\left(\frac{\partial F^1}{\partial z}\right) = \frac{2F^+ - F^0}{\delta t/2} - (-1)^k\left(\frac{\partial F^0}{\partial z}\right) \tag{31}$$

$$\zeta^1 - \frac{\partial}{\partial z}(rF^1) = 0 \quad \text{at } S_k \ (k = 1, 2).$$

The fourth iteration step at $t_0 + \delta t$ computes for the function ψ^1 in the volume of the film for given values of F^1 and ζ^1. In this case the equation can be written as follows:

$$\frac{\psi^1}{\delta t/2} - \left(\frac{\partial^2 \psi^1}{\partial z^2}\right) = \frac{2\psi^+ - \psi^0}{\delta t/2} - \left(\frac{\partial^2 \psi^0}{\partial z^2}\right) \tag{32}$$

with usual boundary conditions on the axis of the revolution and on the spherical solid surface. From eqs (22) and (26) we can obtain the boundary condition on the liquid–gas interfaces

$$\frac{\psi^1}{\delta t/2} + (-1)^k\left(\frac{\partial \psi^1}{\partial z}\right) = \frac{2\psi^+ - \psi^0}{\delta t/2} + (-1)^k\left(\frac{\partial \psi^0}{\partial z}\right)$$

$$\text{at } S_k \ (k = 1, 2). \tag{33}$$

Equations (30)–(33) are solved numerical using the second-order interpolation of the functions on z direction and modified Thomas band matrix method [cf. Jennings (1977)].

The mapping of the numerical grid from the curvilinear coordinate system of revolution onto the r, z-plane in the vicinity of the particle is shown in Fig. 1(b).

5. NUMERICAL RESULTS AND DISCUSSIONS

5.1. *Velocity and pressure distribution*

Considering the coordinate system sketched in Fig. 1(a), the numerical results plotted in Figs 2–9 represent a situation where the lower surface S_1 is positioned at $z_1 = -1.5$, the upper surface S_2 is at $z_2 = 2.0$ and the particle radius is 1.

From experimental investigations, it is known that the dilatational and the shear surface viscosity numbers are of the same order of magnitude for all practically relevant cases. Hence, $K_1 = E_1$ and $K_2 = E_2$ were assumed in all cases. To keep things simple, the upper viscosity numbers were kept constant at $K_2 = E_2 = 0.1$ which corresponds to low surface viscosity or an almost free surface. As a value of 10.0 corresponds to high surface viscosity, K_1 and E_1 were varied between 0.1 and 10.0.

In Fig. 2(a) the velocity vectors in the plane $x = 0$ are plotted for the case, when the lower and upper viscosity numbers are identical, hence $K_1 = E_1 = 0.1$. The relative motion of the particle in the thin liquid film can best be imagined when assuming an external force, i.e. due to an electric or magnetic field, acting upon the particle. Another, perhaps more important effect, which one should bear in mind when talking about the movement of small particles is Brownian motion. At large distances, the velocity of the undisturbed liquid film relative to the particle is 1 and it is interesting to note, that for low surface viscosity numbers the influence of the particle is rather far reaching. Even at a distance of 5 times the particle radius the velocity in the plane $x = 0$ is about 0.5. In contrast, when rising the lower viscosity numbers to $K_1 = E_1 = 10.0$ the disturbances caused by the fluid are damped out very fast, as can be seen in Fig. 2(b). For later discussions of the magnitudes of the drag and torque coefficients, it is important to bear in mind that the boundary layer around the particle is much thinner for higher surface viscosity numbers than for smaller.

In order to demonstrate the three-dimensional character of the problem, Fig. 3 shows the velocity distribution in the plane $z = 0$ which is of course symmetrical to the plane $x = 0$ as can be seen from eq. (11). The low velocity gradients indicate that this plot refers to the same values of K_1 and E_1 as in Fig. 2(a). The pressure distributions which correspond to the velocity field of Fig. 2(a) and (b) are plotted in Fig. 4(a) and (b), respectively, for $-3 < y < 3$. The high pressure gradients in Fig. 4(a), when looking at the region directly below the particle, are only due to the smaller distance to the surface when compared to the region above the solid sphere. Figure 4(b) illustrates the additional influence of the higher surface viscosity numbers. Here, the effect is as pronounced as expected, which could not be seen from the velocity plots. The pressure distribution corresponding to Fig. 3 is shown in Fig. 5, which is a confirmation of the expected antisymmetric character of the pressure in this plane.

The results for the same variations of the lower viscosity numbers K_1 and E_1 as before for the case of a rotating particle are shown in Figs 6 and 7. The velocity in the plane $z = 0$ has three components and the flow is not symmetric. Again a small effect of the distance of the particle from the surface and a large effect of the surface viscosity numbers can be realized when comparing the plots. The absolute values for the pressure are of course smaller than in the previous case except for the region very close to the particle, where the velocity gradients are of the same order of magnitude as before. The smaller influence of the rotating particle in the surrounding liquid can best be seen from the pressure distribution in the plane $z = 0$ in Fig. 8.

Clearly, the presented pressure distributions will lead to deformed interfaces which are plotted in Fig. 9(a) and (b) for the moving and the rotating particle, respectively. In both cases the interfaces have low

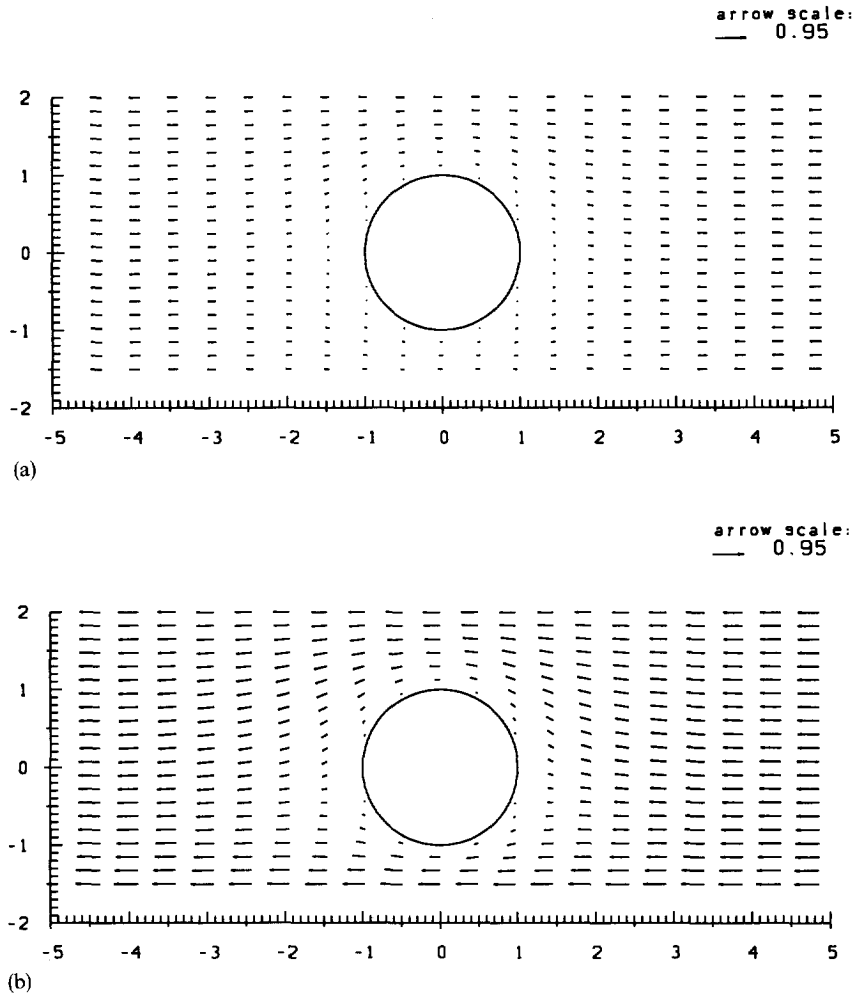

Fig. 2. Velocity field for a spherical particle moving in the plane $x = 0$ for $z_1 = -1.5$ and $z_2 = 2.0$, $K_2 = 0.1$ and $E_2 = 0.1$, and two different values of the lower surface viscosity numbers: (a) $K_1 = 0.1$ and $E_1 = 0.1$, (b) $K_1 = 10.0$ and $E_1 = 10.0$.

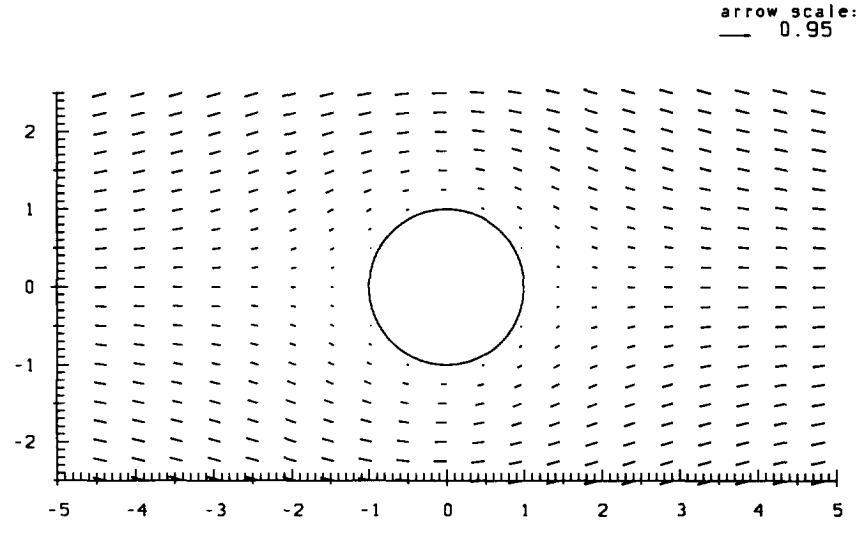

Fig. 3. Velocity field for a spherical particle moving in the plane $z = 0$ for $z_1 = -1.5$ and $z_2 = 2.0$, $K_1 = 0.1$ and $E_1 = 0.1$, $K_2 = 0.1$ and $E_2 = 0.1$.

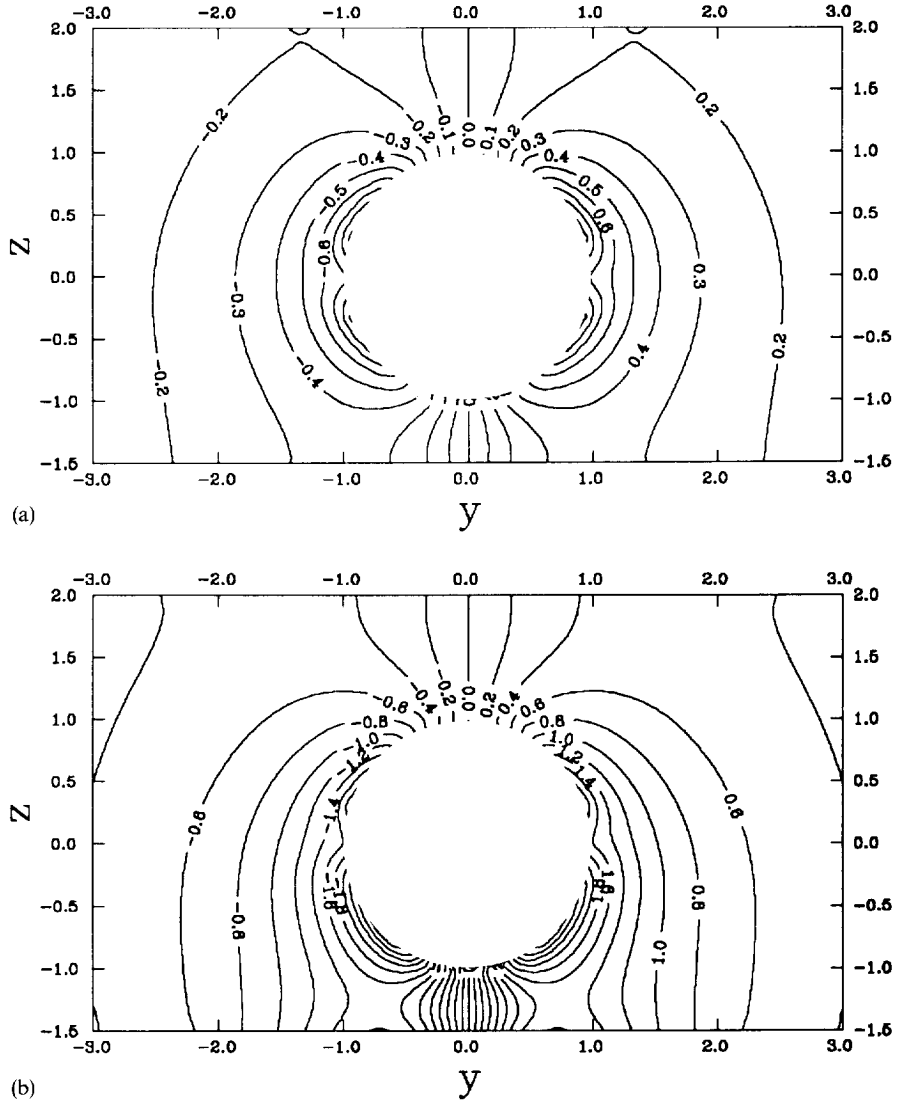

Fig. 4. Pressure distribution for a spherical particle moving in the plane $x = 0$ for $z_1 = -1.5$, $z_2 = 2.0$, $K_2 = 0.1$ and $E_2 = 0.1$ and two different values of the lower surface viscosity numbers: (a) $K_1 = 0.1$ and $E_1 = 0.1$, (b) $K_1 = 10.0$ and $E_1 = 10.0$.

viscosity numbers. The absolute value of the deformation is proportional to the capillary number. In these plots the deformation is however enlarged, in order to give a better impression of the shape of the deformed surface. The numerical solution and the definitions (9) ensure that the film thickness increases before the leading edge and decreases behind the trailing edge of the solid particle in the case of translational motion, because the pressure inside the film is greater before the particle than behind it. In the case of rotation, the shape of the interfaces is more attractive because the particle drags the liquid and the pressure distribution inside the film is very complicated. In both cases the

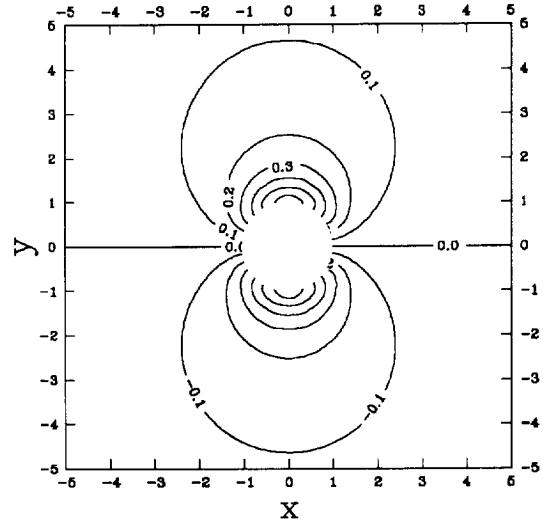

Fig. 5. Pressure distribution for a spherical particle in the plane $z = 0$ for $z_1 = -1.5$ and $z_2 = 2.0$, $K_1 = 0.1$ and $E_1 = 0.1$, $K_2 = 0.1$ and $E_2 = 0.1$.

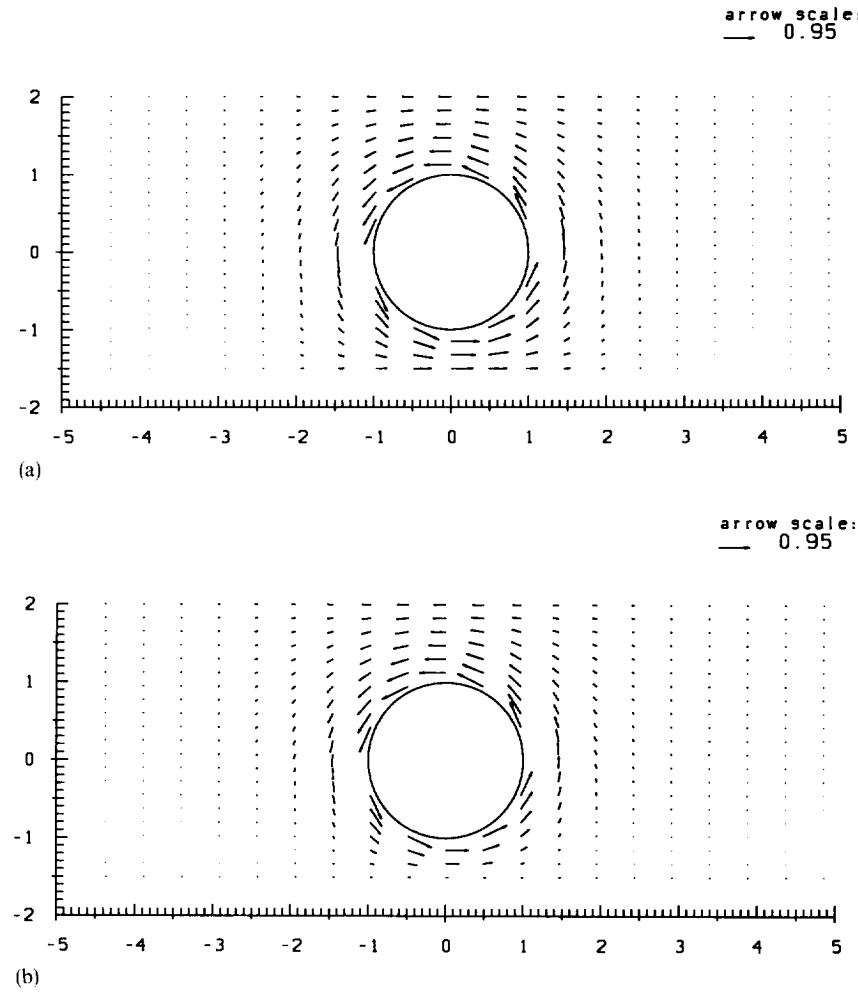

Fig. 6. Velocity field for a spherical particle rotating in the plane $x = 0$ for $z_1 = -1.5$, $z_2 = 2.0$, $K_2 = 0.1$ and $E_2 = 0.1$ and two different values of the lower surface viscosity numbers: (a) $K_1 = 0.1$ and $E_1 = 0.1$, (b) $K_1 = 10.0$ and $E_1 = 10.0$.

absolute value of the disturbances on the far interface is less than on the near interface.

5.2. *Drag and torque coefficients*

The most interesting outcome of our analysis is the influence of the surface viscosity numbers and the distance of the particle from the interface on the drag and torque coefficients as defined by eqs (14)–(16). This could eventually be the basis for the computation of the diffusion coefficient for small particles when moving parallel to an interface of arbitrary viscosity. Besides a better understanding of the behaviour of, i.e. magnetic suspensions under the influence of a magnetic field as used in some coating applications can be achieved.

Figure 10 shows the drag coefficient f for a particle with radius 1 moving in the centre of a liquid film ($m = 0$) for four different film thicknesses of (a) 2.2, (b) 2.4, (c) 3.0 and (d) 4.0. The surface viscosity numbers are kept identical at the upper and lower surface and varied from 0.1 to 10.0. In all cases, the absolute value of the drag coefficient increases with increasing surface viscosity numbers. However, for high surface viscosity numbers the absolute value of the drag coefficient is higher for thinner films, whilst for surface viscosity numbers below approximately 2, particles in thinner films apparently experience less drag than in thick liquid layers. This can be explained by the fact, that at high surface viscosity numbers the influence of the surface is dominating, hence the particle gets slowed down the more, the closer it is to the "rigid" wall. If the surface viscosity numbers are low, then the mass of the liquid which is influenced by the particle through friction is the governing effect. Therefore, in thinner liquid layers, when less liquid is present in the vicinity of the particle, the drag reduces. Apparently, there is a critical value of the surface viscosity numbers of about 1.8, at which the nature of the dominating effect changes. Furthermore, it is worthwhile to note that the absolute value of the drag coefficient reaches almost exactly the value for Stokes' solution of a particle moving in a unbounded liquid ($f = -6$) at this critical surface viscosity numbers.

For the case of particle rotating in the centre plane of a stationary liquid layer ($f = 0$) of varying thick-

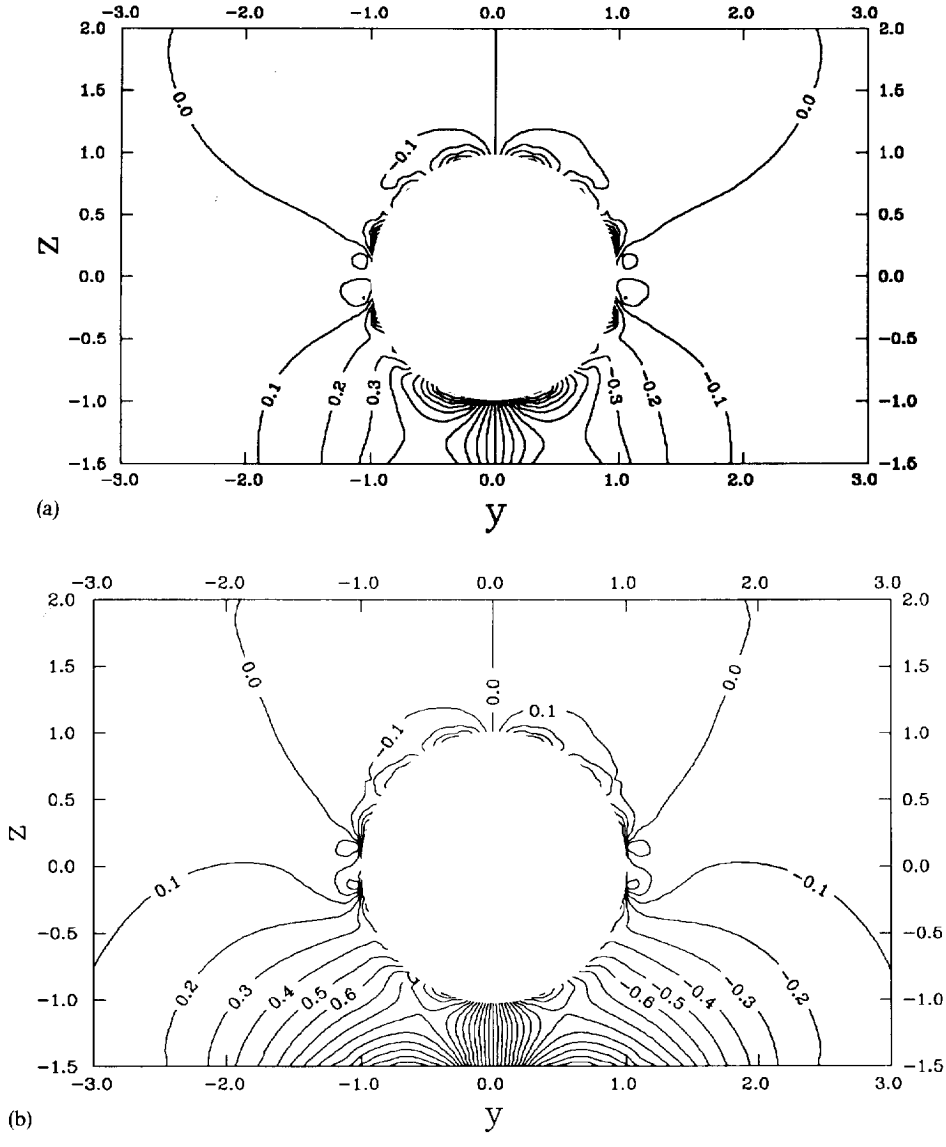

Fig. 7. Pressure distribution for a spherical particle in the plane $x = 0$ for $z_1 = -1.5$, $z_2 = 2.0$, $K_2 = 0.1$ and $E_2 = 0.1$ and two different values of the lower surface viscosity numbers: (a) $K_1 = 0.1$ and $E_1 = 0.1$, (b) $K_1 = 10.0$ and $E_1 = 10.0$.

ness [(a) 2.2, (b) 2.4, (c) 3.0 and (d) 4.0 as before], the torque coefficient is plotted in Fig. 11. Let us first look at curve (a), where the distance of the particle from the interfaces is of the same order of magnitude as the thickness of the velocity boundary layer around the rotating particle. In this case the influence of the surface properties is very pronounced and the torque coefficient can even reach higher values than Kirchhoff's solution for an unbounded liquid ($m = 8$). In all other cases m is less than 8 and the torque coefficient generally decreases with decreasing surface viscosity numbers and increasing film thickness. Whilst the former effect is as expected, the latter

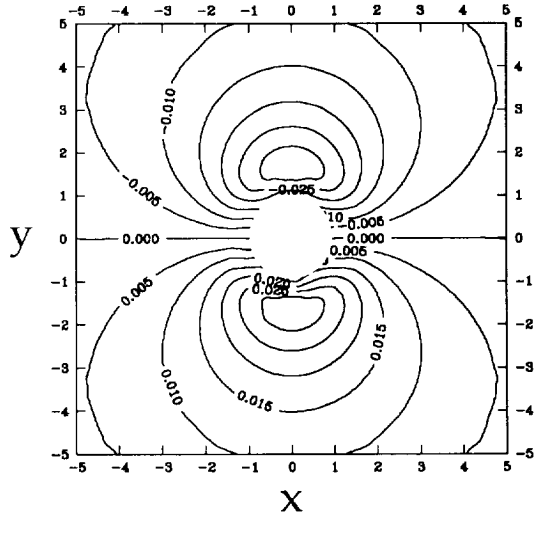

Fig. 8. Pressure distribution for a spherical particle in the plane $z = 0$ for $z_1 = -1.5$ and $z_2 = 2.0$, $K_1 = 0.1$ and $E_1 = 0.1$, $K_2 = 0.1$ and $E_2 = 0.1$

requires a somewhat closer look. When interpreting the influence of the film thickness two effects have to be taken into account:

- the further away the particle is from the surface, the smaller will be the influence of the surface viscosity and hence the absolute value of the torque coefficient should drop;
- however, an increasing film thickness means, that the particle is surrounded by more liquid and hence the torque coefficient should increase and reach Kirchhoff's solution.

From the curves (b)–(d) in Fig. 11 one can conclude, that the absolute magnitude of the limited film thickness is larger than the effect of the increased surface viscosity, as m is smaller than 8. However, in the range of film thicknesses under consideration, the change of the influence of the surface viscosity is stronger than the effect of the additional liquid surrounding the particle when increasing the film thickness. Hence, the torque coefficient drops for thicker liquid layers down to certain value at which the effect reverses and will eventually for very thick films reach Kirchhoff's solution.

Another interesting question is the behaviour of drag and torque when the particle is situated outside of the center plane of the film. Figures 12 and 13 refer to a situation where an absolute film thickness of 4 is assumed and the distance of the particle center from the upper interface z_2 is varied from 1.04 to 2.0. The surface viscosity numbers on both surfaces are 0.1, 1.0 and 10.0 in the cases (a)–(c), respectively. One has to remember, that our investigation is still limited to elementary motion, meaning that the moving particle is not "allowed" to rotate although the induced torque would induce such secondary motions. This is necessary to single out the effects which govern the realistic situation where translational and rotational movement are present simultaneously. Figure 12(a) shows the drag coefficient for a moving particle. For low and moderate values of the surface viscosity number the drag coefficient remains virtually constant except for the case when the particle gets very close to the

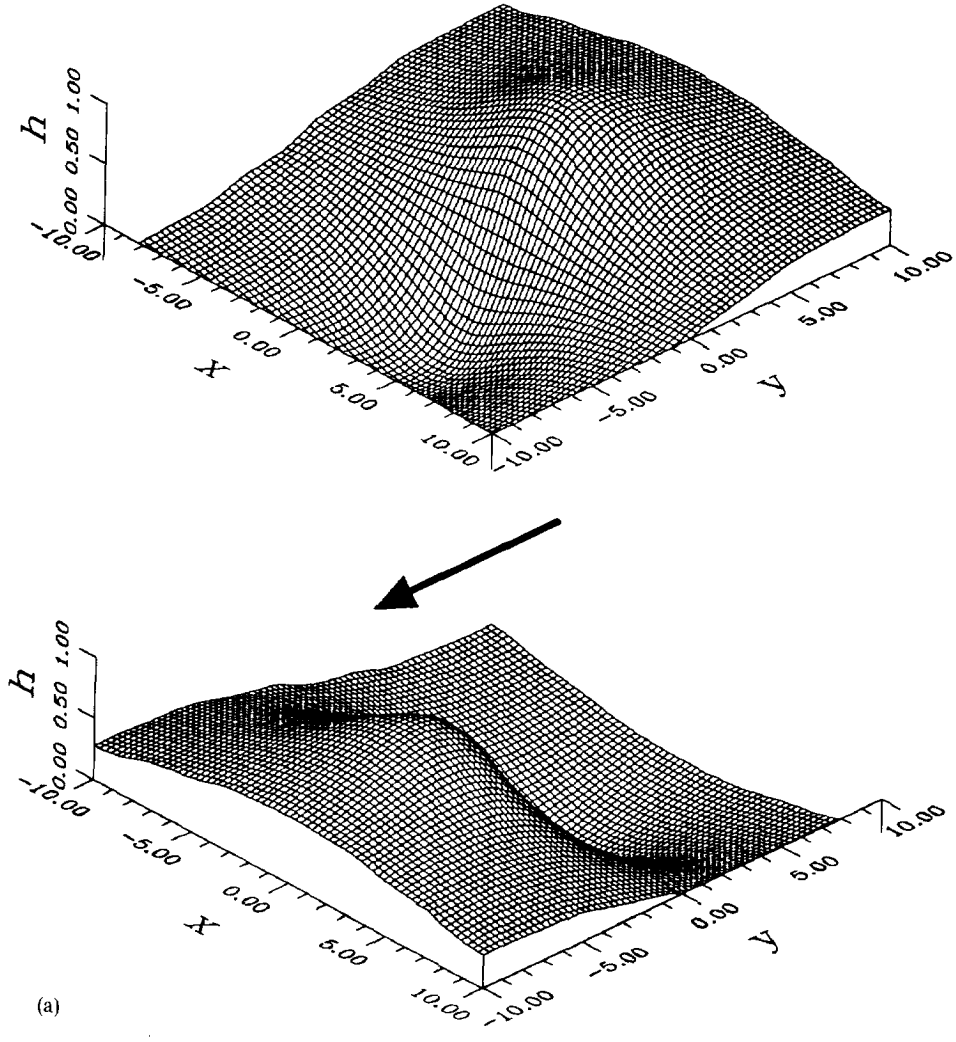

Fig. 9. (a)

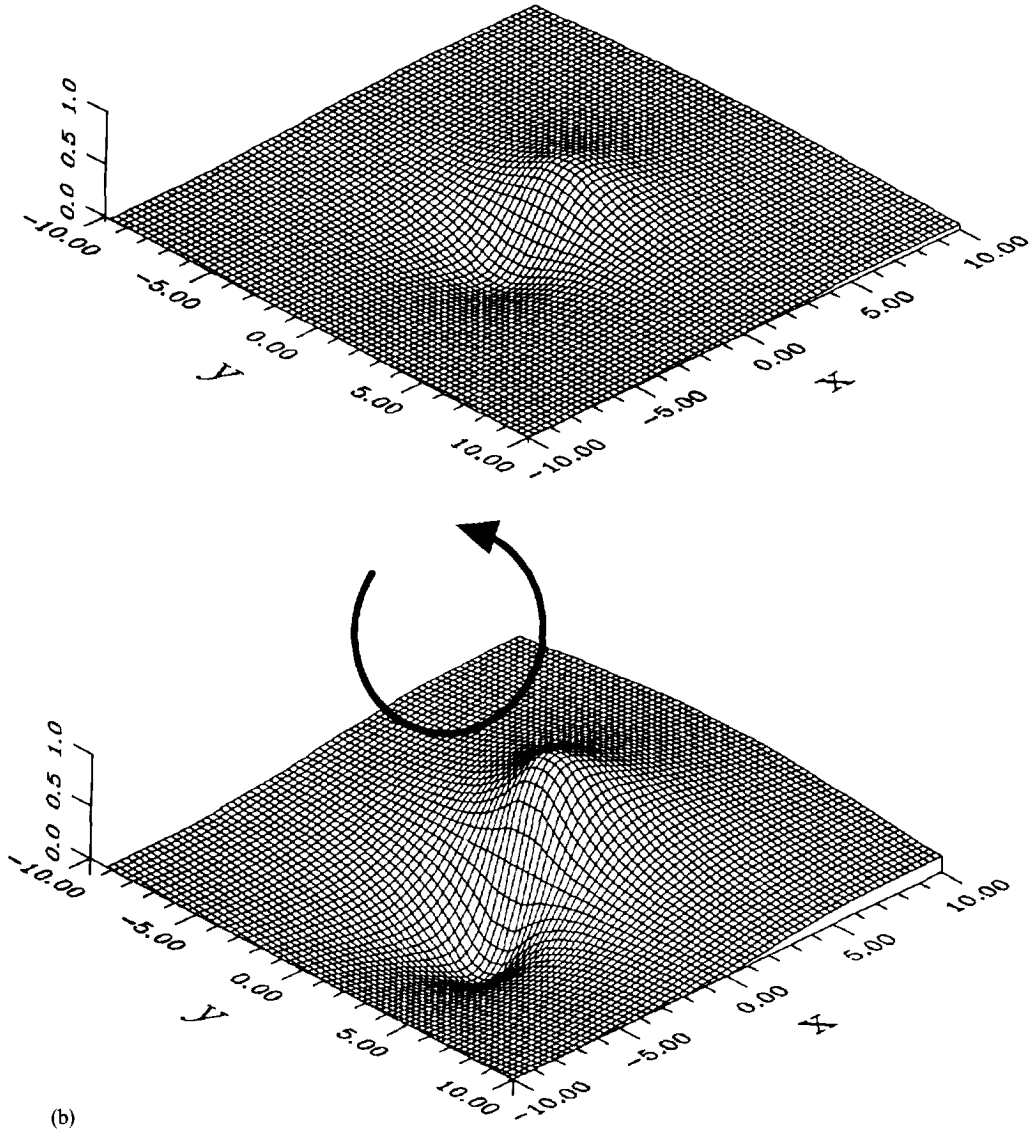

Fig. 9. Disturbances of the interface contours for the film boundaries for $z_1 = -1.5$ and $z_2 = 2.0$, $K_1 = 0.1$ and $E_1 = 0.1$, $K_2 = 0.1$ and $E_2 = 0.1$: (a) the case of moving particle; (b) the case of rotating sphere.

interface, so that the amount of liquid which slows the particle down is substantially reduced on one side. At high values of K_k and E_k the effect is opposite because then the "rigid" wall is dragging the particle. The behaviour of the torque coefficient appears to be quite clear when looking at the curves for low and moderate viscosity (a) and (b). When the particle is in the centre plane ($z_2 = 2$), m is of course zero. When the particle is closer to the wall, the drag on both sides of the particle is different and hence a certain torque is acting on the particle. The negative sign of the torque indicates that for low and moderate surface viscosity numbers the drag on the side which is closer to the interface is lower. For $K_k = E_k = 10.0$ the effect is similar down to 1.4 but then the value changes to positive values, indicating that for small distances the drag on the side closer to the high viscous interface is greater than on the side where the viscous interface is further away.

For a rotating particle, understanding the behaviour of the drag coefficient is straightforward. From Fig. 13(a) one can see, that starting from a value of $f = 0$, when the particle rotates in the center of the plane ($z_2 = 2$), f increases slowly when the particle approaches the wall. Then, at $z_2 = 1.1$ there is a very steep increase for all three different viscosity numbers. The higher the surface viscosity number is, the longer remains f approximately constant and the steeper is the final drop. From the plots of the velocity field we know, that for high viscosities the boundary layer is thinner, hence the interaction with the interface is important only at small distances and because of the higher gradient the effect in this region has to be stronger than for lower viscosity numbers. The torque coefficient plotted in Fig. 13(b) is for all particle positions higher for larger viscosity numbers as expected. When the particle gets closer to the wall it can acceler-

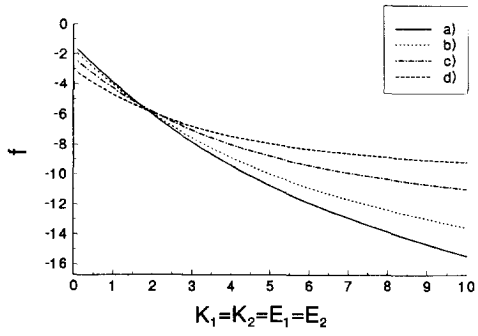

Fig. 10. Influence of the surface viscosity numbers on the drag coefficient in the case of moving particle: (a) $z_2 = -z_1 = 1.1$, (b) $z_2 = -z_1 = 1.2$, (c) $z_2 = -z_1 = 1.5$ and (d) $z_2 = -z_1 = 2.0$.

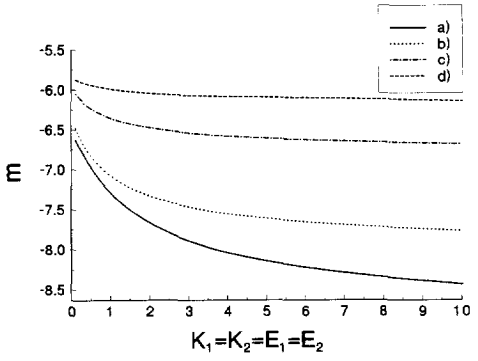

Fig. 11. Influence of the surface viscosity numbers on the torque coefficient in the case of rotating sphere: (a) $z_2 = -z_1 = 1.1$, (b) $z_2 = -z_1 = 1.2$, (c) $z_2 = -z_1 = 1.5$ and (d) $z_2 = -z_1 = 2.0$.

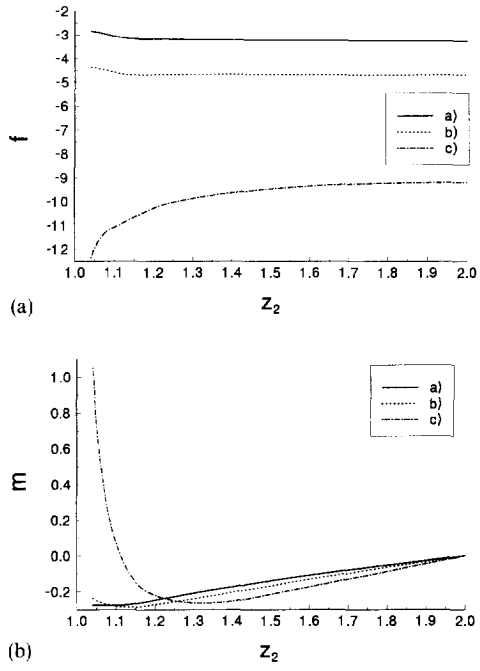

Fig. 12. (a) Dependence of the drag coefficient in the case of a moving particle on the distance from the upper liquid–gas interface: (i) $K_1 = E_1 = K_2 = E_2 = 0.1$, (ii) $K_1 = E_1 = K_2 = E_2 = 1.0$, (iii) $K_1 = E_1 = K_2 = E_2 = 10.0$. In all cases the dimensionless film thickness is 4. (b) Dependence of the torque coefficient in the case of a moving particle on the distance from the upper liquid–gas interface: (i) $K_1 = E_1 = K_2 = E_2 = 0.1$, (ii) $K_1 = E_1 = K_2 = E_2 = 1.0$, (iii) $K_1 = E_1 = K_2 = E_2 = 10.0$. In all cases the dimensionless film thickness is 4.

ate the small amount of remaining liquid between the particle and the interface more and more easily, so that the torque coefficient finally drops. However, as the absolute value of m is smaller than 8 in the whole region, the particle experiences less torque than in unbounded fluid.

5.3. *The stationary motion*

The realistic behaviour of a particle moving under the influence of a buoyancy force along the Oy axis can be described by a superposition of the two elementary motions considered before. For a translational motion with drag coefficient f_m, torque coefficient m_m and stationary translation velocity V_{st} and a rotation around the Ox axis with drag coefficient f_r, torque coefficient m_r and stationary angular velocity ω_{st}, eq. (8) has the following form:

$$f_m \pi\eta a V_{st} + f_r \pi\eta a^2 \omega_{st} = -\frac{4}{3}\pi a^3 \Delta\rho\, g$$
$$m_m \pi\eta a^2 V_{st} + m_r \pi\eta a^3 \omega_{st} = 0 \qquad (34)$$

where g is the acceleration due to gravity and $\Delta\rho$ is the difference of the densities of particle and liquid. From eqs (35) we compute V_{st} and ω_{st} of a particle in a viscous liquid film for the same conditions as in Figs 12 and 13. The velocities in Fig. 14 were normalized with Stokes' solution for the same particle in an unlimited fluid:

$$Stokes = \frac{2}{9}\frac{a^2 \Delta\rho\, g}{\eta}. \qquad (35)$$

Figure 14(a) reveals that for high surface viscosity numbers the particle moves considerably slower than in an unbounded liquid. In contrast, for low and moderate values of K_k and E_k the velocity is up to two times larger. If the particle is very close to the wall it can get even further accelerated. However, in all cases the change in surface viscosity has a strong global effect on the whole film and only directly at the surface additional effects occur. The scaled angular velocity plotted in Fig. 14(b) shows in general less pronounced effects, but for high surface viscosity numbers the direction of rotation can change, when the particle is very close to the surface. This might for example be important for understanding some special effects in curtain coating in the area where the falling film hits the web and hence the viscosity of the surface changes dramatically in one point.

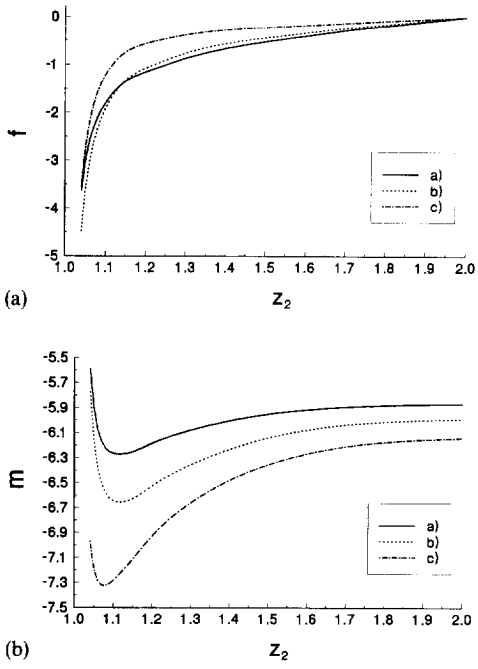

Fig. 13. (a) Dependence of the drag coefficient in the case of a rotating sphere on the distance from the upper liquid–gas interface: (i) $K_1 = E_1 = K_2 = E_2 = 0.1$, (ii) $K_1 = E_1 = K_2 = E_2 = 1.0$, (iii) $K_1 = E_1 = K_2 = E_2 = 10.0$. In all cases the dimensionless film thickness is 4. (b) Dependence of the torque coefficient in the case of a rotating sphere on the distance from the upper liquid–gas interface: (i) $K_1 = E_1 = K_2 = E_2 = 0.1$, (ii) $K_1 = E_1 = K_2 = E_2 = 1.0$, (iii) $K_1 = E_1 = K_2 = E_2 = 10.0$. In all cases the dimensionless film thickness is 4.

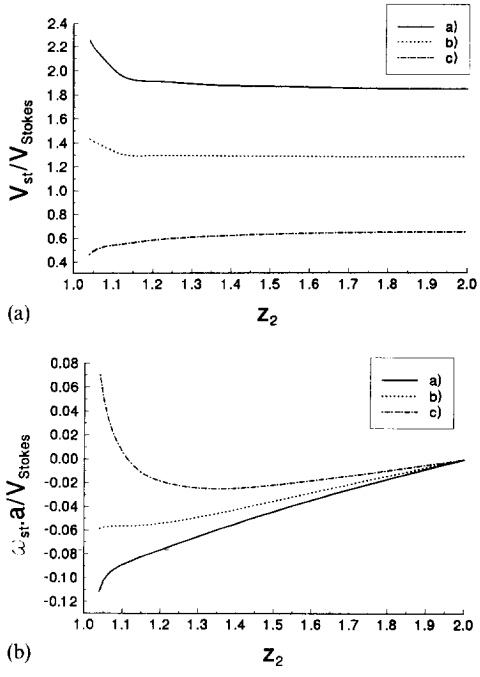

Fig. 14. (a) Influence of the surface viscosity numbers and distance from the upper liquid–gas interface on the stationary translation velocity V_{st} in the presence of the buoyancy force: (i) $K_1 = E_1 = K_2 = E_2 = 0.1$, (ii) $K_1 = E_1 = K_2 = E_2 = 1.0$, (iii) $K_1 = E_1 = K_2 = E_2 = 10.0$. In all cases the dimensionless film thickness is 4. (b) Influence of the surface viscosity numbers and distance from the upper liquid–gas interface on the stationary angular velocity ω_{st} in the presence of the buoyancy force: (i) $K_1 = E_1 = K_2 = E_2 = 0.1$, (ii) $K_1 = E_1 = K_2 = E_2 = 1.0$, (iii) $K_1 = E_1 = K_2 = E_2 = 10.0$. In all cases the dimensionless film thickness is 4.

6. CONCLUSION

The presented model for the computation of the drag force and the torque, acting on a solid spherical particle moving in a thin liquid layer allows the investigation of the influence of surface viscosity effects and the film thickness on the particle movement. It can be applied for small Reynolds and capillary numbers, when the film is bounded by viscous liquid–gas interfaces which obey the Boussinesq–Scriven constitutive law.

From the analysis performed within the scope of this paper the following conclusions can be drawn:

- Whilst the drag force, acting on the particle, tends to be lower in liquid layers than in an unbounded liquid in the absence of surfactants, the presence of, i.e. protein isolates can increase the drag coefficient by almost an order of magnitude.
- Although the absolute effect of the surface viscosity is already very impressive, it is even more interesting that the change of the drag force acting on the particle does virtually not depend on its position within the film. Hence, changing the surface viscosity means changing the global properties of the whole film.
- Following on from this, it was found that particles moving in a liquid film, i.e. due to the presence of a buoyancy force, can move twice as fast or twice as slow as in an unbounded liquid, depending on the surface viscosity number.
- Finally, some special effects which occur very close to the viscous interface, such as the possibilities of different directions of rotation of the particle, depending on the surface viscosity and the distance of the particle from the surface could be identified. These might be of considerable importance for technological applications.

Acknowledgements—We are indebted to Professor I. B. Ivanov for the most helpful discussions. Besides, we are grateful for the advice provided by Dr. H. Raszillier. This work was supported financially by the "Volkswagen–Stiftung". The authors gratefully acknowledge this support of their collaborative research.

REFERENCES

Boussinesq, M. J., 1913, Sur l'éxistance d'une viscosité' superficielle, dans la mince couche de transition separant un liquide d'une autre fluide contigue. *Ann. Chim. Phys.* **29**, 349–357.

Brebbia, C. A., 1978, *The Boundary Element Method for Engineers*. Pentech Press, London.

Brenner, H., 1973, Rheology of a dilute suspension of axisymmetric Brownian particles. *Int. J. Multiphase Flow* **1**, 195–341.

Brenner, H. and Leal, G. L., 1982, Conservation and constitutive equations for adsorbed species undergoing surface diffusion and convection at a fluid-fluid interface. *J. Colloid Interface Sci.* **88**, 136–184.

Cooley, M. D. A. and O'Neill, M. E., 1968, On the slow rotation of a sphere about a diameter parallel to a nearby plane wall. *J. Inst. Math. Appl.* **4**, 163–173.

Davis, R. H., 1993, Microhydrodynamics of particulate suspensions. *Adv. Colloid Interface Sci.* **43**, 17–50.

Dean, W. R. and O'Neill, M. E., 1963, A slow motion of viscous liquid caused by a slowly rotating solid sphere. *Mathematika* **10**, 13–24.

Edwards, D. A., Brenner, H. and Wasan, D. T., 1991, *Interfacial Transport Processes and Rheology*. Butterworth–Heinemann, Boston.

Einstein, A., 1956, *Investigations of the Theory of the Brownian Movement*. Dover, New York.

Faxén, H., 1921, Dissertation. Uppsala University.

Fletcher, C. A. J., 1984, *Computational Galerkin Methods*. Springer, New York.

Fletcher, C. A. J., 1991a, *Computational Techniques for Fluid Dynamics, Vol.* I. Springer, New York.

Fletcher, C. A. J., 1991b, *Computational Techniques for Fluid Dynamics, Vol.* II. Springer, New York.

Goldman, A. J., Cox, R. G. and Brenner, H., 1967, Slow viscous motion of a sphere parallel to a plane wall. *Chem. Engng Sci.* **22**, 637–651.

Goldsmith, H. L. and Mason, S. G., 1967, The microrheology of dispersions, in *Rheology: Theory and Applications, Vol.* 4 (Edited by F. R. Eirich), pp. 85–250. Academic Press, New York.

Hadamard, J. S., 1911, Mouvement permenent lent d'une sphere liquide et visqueuse dans un liquide visqueux. *Comp. Rend. Acad. Sci* (Paris) **152**, 1735–1738.

Happel, J. and Brenner, H., 1965, *Low Reynolds Number Hydrodynamics with Special Applications to Particulate Media*. Prentice-Hall, New York.

Hetsroni, G., 1982, *Handbook of Multiphase System* (Edited by G. Hetsroni). Hemisphere, Washington.

Hunter, R. J., 1987, *Foundation of Colloid Science, Vol.* I. Clarendon Press, Oxford.

Hunter, R. J., 1989, *Foundation of Colloid Science, Vol.* II. Clarendon Press, Oxford.

Jeffery, G. B., 1922, The motion of ellipsoidal particles immersed in a viscous fluid. *Proc. R. Soc. London* **A102**, 161–179.

Jennings, A., 1977, *Matrix Computations for Engineers and Scientists*. Wiley, Chichester.

Joly, M., 1964, Surface viscosity, in *Recent progress in Surface Science, Vol.* I (Edited by J. F. Danielli, K. G. A. Pankhurst and A. C. Riddiford), pp. 1–50. Academic Press, New York.

Kim, S. and Karrila, S. J., 1991, *Microhydrodynamics: Principles and Selected Applications*. Butterworth–Heinemann, Boston.

Kirchhoff, G., 1876, The slow rotation of a sphere in a viscous fluid, in Lamb, H. (1945) *Hydrodynamics*. Dover, New York.

Lebedev, A. A., 1916, *Zhur. Russ. Fiz. Khim.* **48**.

Levich, V. G., 1962, *Physicochemical Hydrodynamics*. Prentice-Hall, Englewood Cliff, NJ.

Lorentz, H. A., 1906, *Abhandl. Theoret. Phys.* **1**, 23.

Malhotra, A. K. and Wasazn, D. T., 1987, Effects of surfactant adsorption–desorption kinetics and interfacial rheological properties on the rate of drainage of foam and emulsion films. *Chem. Engng Commun.* **55**, 95–128.

O'Neill, M. E., 1964, A slow motion of viscous liquid caused by a slowly moving solid sphere. *Mathematika* **11**, 67–74.

O'Neill, M. E. and Stewartson, K., 1967, On the slow motion of a sphere parallel to a nearby plane wall. *J. Fluid Mech.* **27**, 705–724.

O'Neill, M. E. and Ranger, K. B., 1979, Rotation of a sphere in two phase flow. *Int. J. Multiphase Flow* **5**, 143–148.

Ranger, K. B., 1978, The circular disk straddling the interface of a two-phase flow. *Int. J. Multiphase Flow* **4**, 263–277.

Russel, W. B., Saville, D. A. and Schowalter, W. R., 1989, *Colloid Dispersions*. Cambridge University Press, Cambridge.

Rybczynski, W., 1911, *Bull. Intern. Acad. Sci.* Cracovie (Ser. A).

Scriven, L. E., 1960, Dynamics of a fluid interface. *Chem. Engng Sci.* **12**, 98–108.

Shapira, M. and Haber, S., 1988, Low Reynolds number motion of a droplet between two parallel flat plates. *Int. J. Multiphase Flow* **14**, 483–506.

Shapira, M. and Haber, S., 1990, Low Reynolds number motion of a droplet in shear flow including wall effects. *Int. J. Multiphase Flow* **16**, 305–321.

Silvey, A., 1916, The fall of mercury droplets in a viscous medium. *Phys. Rev.* **7**, 106–111.

Sternling, C. V. and Scriven, L. E., 1959, Interfacial turbulence: Hydrodynamic instability and the Marangoni effect. *A.I.Ch.E. J.* **5**, 514–523.

Stokes, G. G., 1851, On the effect of the internal friction of fluids on the motion of a pendulum. *Trans. Cambridge Phil. Soc.* **1**, 104–106.

Uijttewaal, W. S. J., 1993, On the motion of particles in bounded flows. Applications in hemorheology. *Ph.D. thesis*, CIP-Gegevens Koninklijke Bibliotheek, Den Haag, Nederlands.

Uijttewaal, W. S. J., Nijhof, E.-J. and Heethaar, R. M., 1993, Droplet migration, deformation, and orientation in the presence of a plane wall: A numerical study compared with analytical theories. *Phys. Fluid A* **5**(4), 819–825.

Wakiya, S., 1956, *Res. Rep. Fac. Engng* **5**, Niigata University, Japan.

Zapryanov, Z., Malhotra, A. K., Aderangi, N. and Wasan, D. T., 1983, Emulsion stability: An analysis of the effects of bulk and interfacial properties on film mobility and drainage rate. *Int. J. Multiphase Flow* **9**, 105–129.